



Glycosidase- and β -lactamase-like activity of dinuclear copper(II) patellamide complexes[☆]



Peter Comba^{*}, Annika Eisenschmidt, Nora Kipper, Jasmin Schießl

University of Heidelberg, Institute of Inorganic Chemistry and Interdisciplinary Center for Scientific Computing, Im Neuenheimer Feld 270, D-69120 Heidelberg, Germany

ARTICLE INFO

Article history:

Received 20 November 2015

Received in revised form 27 January 2016

Accepted 10 February 2016

Available online 13 February 2016

Keywords:

Cyclic peptides

Copper(II) complexes

Ascidian

Prochloron

Glycosidase

Lactamase

ABSTRACT

Prochloron, a blue-green algae belonging to ancient prokaryotes, produces, like other cyanobacteria, cyclic *pseudo*-peptides, which are also found in its obligate symbiont *ascidiae* (*Lissoclinum patellum*). Although research has focused for some time on the putative metabolic function of these cyclic peptides, to date it is still not understood. Their role might be connected to the increased concentrations of divalent metal ions, especially Cu^{II} , found in *ascidiae*. Dinuclear copper(II) complexes of cyclic *pseudo*-peptides revealed a broad hydrolytic capacity, including carboanhydrase and phosphatase activity. This study reports their β -lactamase as well as α - and β -glycosidase activity with $k_{\text{cat}} = (11.34 \pm 0.91) \cdot 10^{-4} \text{ s}^{-1}$ for β -lactamase, $k_{\text{cat}} = (1.55 \pm 0.13) \cdot 10^{-4} \text{ s}^{-1}$ for α -glycosidase and $k_{\text{cat}} = (1.22 \pm 0.09) \cdot 10^{-4} \text{ s}^{-1}$ for β -glycosidase activity.

© 2016 Elsevier Inc. All rights reserved.

1. Introduction

Patellamides like ascidiacyclamide or patellamide D (see Fig. 1), are cyclic peptides, naturally produced via a ribosomal pathway by the cyanobacterium *Prochloron* [1,2]. These cyclic *pseudo*-octapeptides are found in high quantities in their obligate symbiont *L. patellum* that moreover exhibits high concentrations of copper(II) compared to the surrounding sea water [3]. The four azole-N as well as the four amide-N atoms are possible donors for metal ion coordination. Due to the low yield of biosynthesis and isolation from natural sources, routes were developed to synthetically produce cyclic *pseudo*-peptides [4–6]. A number of different model peptides were produced, in the following referred to as “pat”, differing foremost in the stereochemistry and azole heterocycles (see Fig. 1), and have been extensively studied towards their copper(II) complexing behavior, exhibiting a preference for dinuclear complexes in the $\text{N}_{\text{Imidazole}}\text{-N}_{\text{Amide}}\text{-N}_{\text{Imidazole}}$ binding site [3]. It could be shown that the dinuclear copper(II) complexes of the synthetic peptides are catalytically active in the physiological pH range as carboanhydrase- and phosphatase-like enzyme models [7,8].

In this study, the dinuclear copper(II) complexes of the cyclic *pseudo*-octapeptides H_4pat^1 and H_4pat^2 (Fig. 2), the solution structures of which are known from a combination of EPR spectroscopy, spectra simulations and molecular modeling, [3,6,9] are investigated concerning their catalytic activity at higher pH values. For that, a hypothetically

catabolic role, namely glycosidase-like activity and a potential antibiotic role as a β -lactamase-like enzyme were chosen.

1.1. Glycoside hydrolases

Glycosyl transfer reactions are essential in biology and were therefore targets for model catalyst research. However, for a long time only substrates with an additional binding site for Lewis acids like Al^{3+} , Zn^{2+} and Fe^{3+} were investigated. Only recently, few studies on dinuclear copper(II) complexes as enzyme models for glycosidase appeared [10–14]. According to their structure, glycosidases are divided in different subfamilies. Most of these have an organic active site responsible for the catalytic glycoside cleavage depicted in Scheme 1. However, the 4th family was shown to be metal ion dependent [15]. As the use of these enzymes for glycosyl transfer reactions is limited by their low availability [16], the design and evaluation of new glycosidase mimics with increased selectivity and reaction yields is desirable [10]. The development of model compounds that catalyze glycosyl transfer reactions can be interesting for the synthesis of carbohydrates, which are needed as food fillers and may also be of interest as antiviral agents or new antibiotics.

1.2. β -lactam hydrolases

Six different subtypes of β -lactam antibiotics, penams, cepheams, monobactams, clavams, penems and carbapenems, are known [17]. Five of them are readily hydrolyzed by metallo- β -lactamases, only monobactams withstand the predominantly dinuclear zinc(II) complexes.

[☆] In memory of Professor Graeme Hanson and his contributions to Bioinorganic Chemistry and Electron Paramagnetic Resonance.

^{*} Corresponding author.

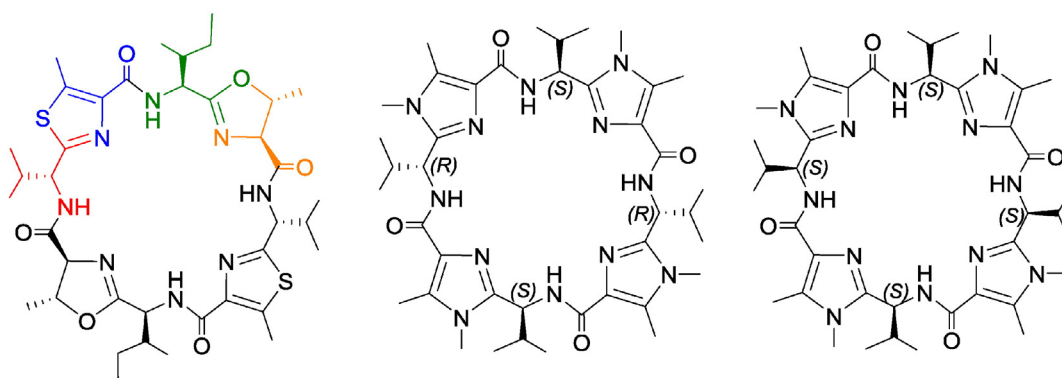


Fig. 1. Ascidiacyclamide and synthetic model ligands H_4pat^1 and H_4pat^2 ; the color code in Ascidiacyclamide shows the amino acid building blocks of one half of the molecule, also relevant in the biosynthesis and showing why these are best named cyclic pseudo-octa-peptides.

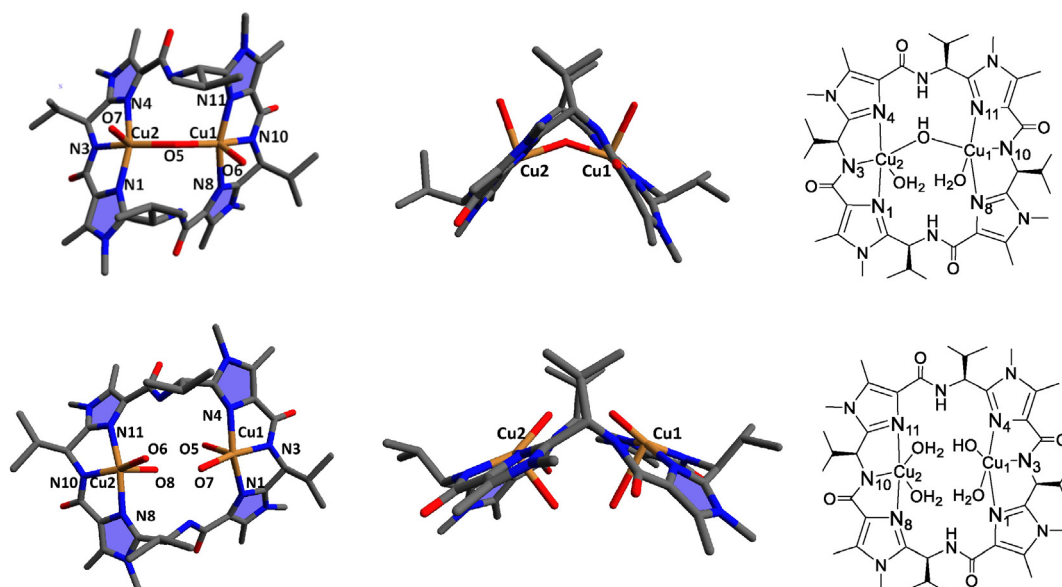


Fig. 2. Computed structures of hydroxido-bridged $[Cu_2(H_2pat^2)(OH)(H_2O)_2]^+$ (1) (top) and $[Cu_2(H_2pat^2)(OH)(H_2O)_3]^+$ (2) (bottom); orange: Cu^{II} , red: O, blue: N.

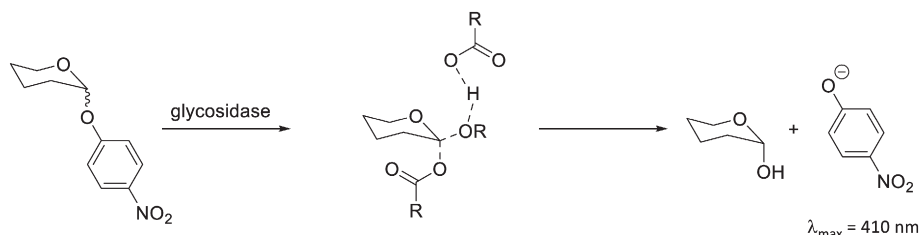
Both zinc(II) ions bind water and, due to their Lewis acidity, decrease its pK_a , resulting in a hydroxido complex. The proposed mechanism of the cleavage is shown in Scheme 2 [17].

Upon cleavage of the amide bond the formerly antibiotic compound cannot bind irreversibly to PBP, which are responsible for the establishment of peptide bonds in murein, a component of the bacterial cell wall. Due to their broad substrate specificity profile and the high activity of class B metallo- β -lactamases, especially towards carbapenems, exhibiting the broadest spectrum of antibiotic activity, current research focuses on understanding this class of enzymes. Profound comprehension of the mechanism and the structures of metallo- β -lactamases might be the foundation for a potential application in bioremediation as well as for drug design [18].

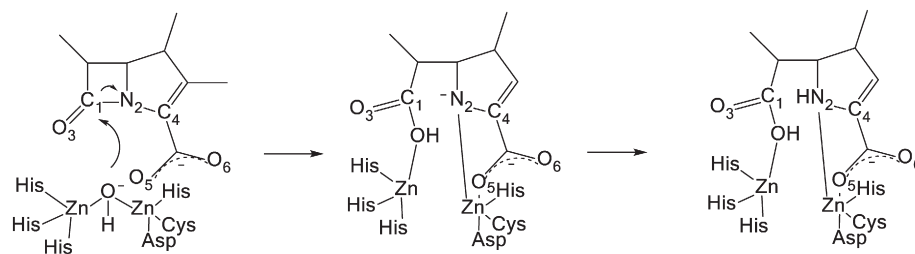
2. Results and discussion

2.1. Syntheses and structures of the dinuclear complexes

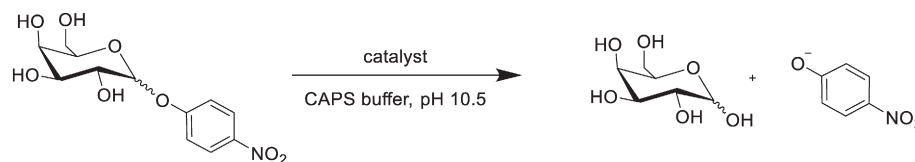
The ligands were obtained as described before [4–6,19]. The geometry of the metal-free ligands was extensively discussed [3]. Analogous to the zinc(II) complexes described above, a hydroxido-bridged conformation of the dicopper(II) complexes of the patellamides was reported [20]. In addition to the μ -hydroxido-bridged coordination mode, a dicopper(II) complex with terminal OH^- donors is also possible and likely to be the catalytically active species, as substrate coordination may be preferred to this active site. These two structures have been computed (see Fig. 2, structural data are given as Supporting Information), and analogous



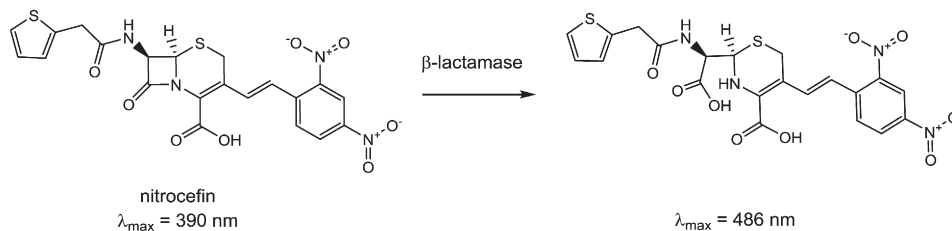
Scheme 1. Schematic representation of the metal ion free glycoside hydrolysis.



Scheme 2. Proposed mechanism of the hydrolysis of β -lactam-antibiotics via NDM-1 (New Delhi Metallo- β -lactamase1) [17,18].



Scheme 3. Catalytic hydrolysis of 4-nitrophenyl-D-galactopyranoside [10].



Scheme 4. Schematic representation of β -lactam hydrolysis.

structures have been identified by EPR spectroscopy [3,6,9]. The major difference between the bridged and unbridged structures **1** and **2** with the same ligand H_4pat^2 is the angle between the two copper(II) centers. The angle between the two sites in **1** is 107° , **2** adopts a different conformation with a 132° angle between the two sites (twist of the imidazole-amide-imidazole-copper planes). This leads to a larger distance between the copper(II) centers (3.98 Å in **1**, 5.23 Å in **2**).

2.2. Glycosidase-like activity

The experimental investigations involved 4-nitrophenyl- α -D-glucopyranoside and 4-nitrophenyl- β -D-glucopyranoside as glycosidase model substrates. Previous experiments with 4-nitrophenyl- α -D-

galactopyranoside as a glycosidase model substrate proved that the hydrolysis product of these highly activated ethers are spectrophotometrically easily detectable (Scheme 3) [10]. (See Scheme 4)

The optimal pH range for the maximum kinetic activity was determined by pH-dependent measurements with a constant catalyst (40 μ M) and substrate concentration (30 mM) in a 0.3: 1.3: 1 mixture of MeCN: buffer: MeOH as solvent; the pH values were controlled by a multicomponent buffer, see Experimental Section. The rate for the uncatalyzed reaction was subtracted to yield the catalytic rate. The pH-dependence of the catalysis rates were measured in steps of 0.5 pH units or smaller from pH = 8.0 to pH = 11.5 for the dicopper(II) complexes **3** and **2** of the cyclic pseudo-octa-peptides H_4pat^1 and H_4pat^2 . The pH profiles are shown in Fig. 3.

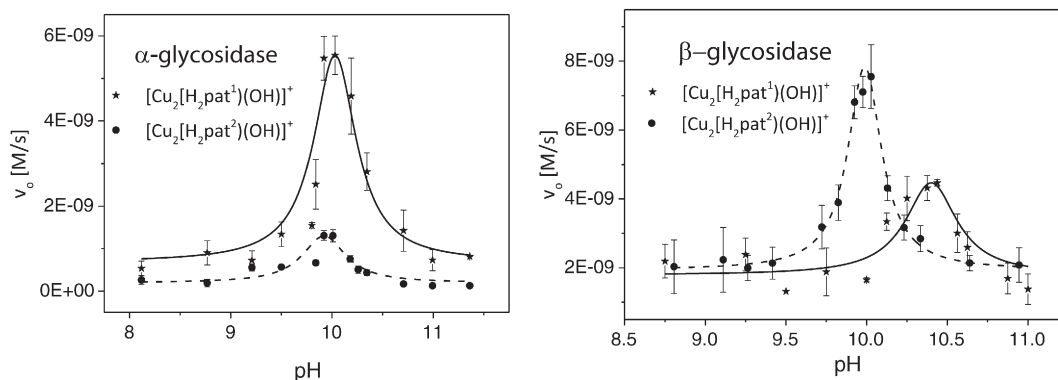


Fig. 3. pH profiles of $[Cu_2(H_4pat^1)(OH)]^+$ (solid) (**3**), $[Cu_2(H_4pat^2)(OH)]^+$ (**2**) (dashed) catalyzed 4-nitrophenyl- α -D-glucopyranoside (left) and 4-nitrophenyl- β -D-glucopyranoside (right) hydrolysis ($c = 10.5$ mM).

Table 1Kinetic data from pH-profiles of $[\text{Cu}_2(\text{H}_2\text{pat}^1)(\text{OH})]^+$ (**3**) and $[\text{Cu}_2(\text{H}_2\text{pat}^2)(\text{OH})]^+$ (**2**) for glycosidase activity and corresponding Michaelis–Menten parameters.

Catalyst		pH _{max}	v _{0,max} [$\times 10^{-9}$ M/s]	pK _{a1}	pK _{a2}	γ	k _{cat} 10 ⁻⁴ [s ⁻¹]	K _M [mM]	k _{cat} /K _M 10 ⁻² [M ⁻¹ s ⁻¹]
α -glyc.	3	10.03	6.19 \pm 0.53	9.86 \pm 0.03	10.20 \pm 0.14	0.1954 \pm 0.0357	1.55 \pm 0.13	4.64 \pm 0.43	3.30 \pm 0.3
	2	9.92	1.11 \pm 0.21	9.73 \pm 0.09	10.09 \pm 0.04	0.1748 \pm 0.0417	0.28 \pm 0.01	1.90 \pm 0.47	1.49 \pm 0.1
β -glyc.	3	10.36	3.36 \pm 0.03	10.19 \pm 0.04	10.53 \pm 0.04	0.2378 \pm 0.0521	1.22 \pm 0.09	3.56 \pm 0.23	3.43 \pm 0.04
	2	9.43	5.86 \pm 0.02	9.21 \pm 0.02	9.64 \pm 0.02	0.2435 \pm 0.0508	1.08 \pm 0.04	2.12 \pm 0.17	5.09 \pm 0.02

All measured data were fitted by a non-linear regression to a Michaelis–Menten model. The determined pH profiles were fitted with Eq. (1), which is based on a model for a diprotic system [21].

$$v_0 = \frac{v_{\max} \left(1 + \frac{\gamma K_{a2}}{[\text{H}^+]} \right)}{\left(1 + \frac{[\text{H}^+]}{K_{a1}} + \frac{K_{a2}}{[\text{H}^+]} \right)} \quad (1)$$

Here, v_0 is the initial and v_{\max} the maximum reaction rate, reached under given conditions. The factor γ is related to the relative activity of the two active species in equilibrium (E^{nS} and $\text{E}^{\text{n-1S}}$); a value of γ less than unity corresponds to a more active E^{nS} adduct and a value larger than one considers the deprotonated adduct $\text{E}^{\text{n-1S}}$ as more active. The rates for the two deprotonation steps pK_{a1} and pK_{a2} are given in Table 1. The velocity $v_{0,\max}$ is defined as the maximum initial rate at given conditions at optimum pH. Measurements at the optimum pH values in dependence of the substrate concentration were also fitted according to a Michaelis–Menten model (see Fig. 4 and Table 1). Here, the concentration of 4-nitrophenyl- α/β -D-glycopyranoside was varied between 1 and 10 mM. The data were fitted to Eq. (2), providing the Michaelis–Menten constant K_M , which was used to determine k_{cat} (Eq. (3)), both summarized in Table 1.

$$v = v_{\max} \frac{[S]_0}{(K_M + [S]_0)} \quad (2)$$

$$k_{\text{cat}} = \frac{v_{\max}}{[K]_0} \quad (3)$$

The α -glycosidase-like model system shows a narrow pH range. The difference of the determined pK_a values is very small and the maximum activities are at pH = 10.03 ($[\text{Cu}_2(\text{H}_4\text{pat}^1)(\text{OH})]^+$, **3**) and 9.92 ($[\text{Cu}_2(\text{H}_4\text{pat}^2)(\text{OH})]^+$, **2**). For the β -glycosidase data, the difference between the determined pK_a values is very small and the maximum activities are at pH = 10.36 ($[\text{Cu}_2(\text{H}_4\text{pat}^1)(\text{OH})]^+$, **3**) and 9.43 ($[\text{Cu}_2(\text{H}_4\text{pat}^2)(\text{OH})]^+$, **2**). The glycosidase-like activity of $[\text{Cu}_2(\text{H}_2\text{pat}^1)(\text{OH})]^+$ (**3**) and $[\text{Cu}_2(\text{H}_2\text{pat}^2)(\text{OH})]^+$ (**2**) are of the same order of

magnitude for α - and β -glycosides. For α -glycosides, the optimal pH is ca. 10 for **3** and **2**, for β -glycosidase the optimal pH is 10.4 for **3** and 9.4 for **2**. The uncatalyzed background rate constants for α - and β -glycosidase are $k_{\text{uncat}} = 0.0135 \cdot 10^{-4} \text{ s}^{-1}$ and $k_{\text{uncat}} = 0.0286 \cdot 10^{-4} \text{ s}^{-1}$, respectively, [22] and this corresponds to rate enhancements $k_{\text{cat}}/k_{\text{uncat}}$ for the pat^1 and pat^2 based catalysts of 115 and 21 for α - and of 43 and 37 for β -glycosidase, respectively. That is, the catalyst with the configuration of the natural product (pat^1) generally is a more efficient catalyst, and this observation was also made for the carboanhydrase and phosphatase activities, i.e. the configuration of the side-chains of the cyclic *pseudo*-octapeptides is of crucial importance [7,8]. Note that the optimum pH value for the catalytic hydrolysis of glycosides of around 10 is outside the physiological range. It is interesting to note here that this is not the case with the carboanhydrase and phosphatase activities which have optimum performance around pH = 7 [7,8]. Glycosidase activity with dicopper(II) complexes has only been studied with a small range of other model systems [10–13]. Interestingly, these also have optimum performance in the range of pH = 10. So far, it has not been studied whether and how this is related to the substrate used. Natural glycosidase activity is reported to be in the range of $K_M = 4\text{--}14 \text{ mM}$ and $k_{\text{cat}} = 0.14\text{--}14 \text{ s}^{-1}$ [30] for α -glycosidase activity (substrate phenyl- α -glycoside) and $K_M = 0.07 \text{ mM}$, $k_{\text{cat}} = 169 \text{ s}^{-1}$ for Agrobacterium β -Glucosidase (substrate: 4-nitrophenyl-D-glucoside) [23].

2.3. β -lactamase-like activity

Similar to the glycosidase activity measurements, the optimal pH range for maximum lactamase activity was determined by pH-dependent measurements with a constant catalyst (5 μM) and substrate concentration (25 μM) in a 1:1 MeCN: buffer mixture as solvent; the pH values were controlled by a multicomponent buffer, see Experimental Section. The pH dependence of the catalysis rates were measured in steps of 0.5 pH units or smaller from pH = 9.0 to pH = 12.0 for the dicopper(II) complexes of the cyclic *pseudo*-octapeptides H_4pat^1 and H_4pat^2 . For $[\text{Cu}_2(\text{H}_2\text{pat}^2)(\text{OH})]^+$ (**2**) no activity could be observed. The initial rates at each pH value were corrected for the corresponding autohydrolysis rates. The pH profile for $[\text{Cu}_2(\text{H}_2\text{pat}^1)(\text{OH})]^+$ (**3**) is

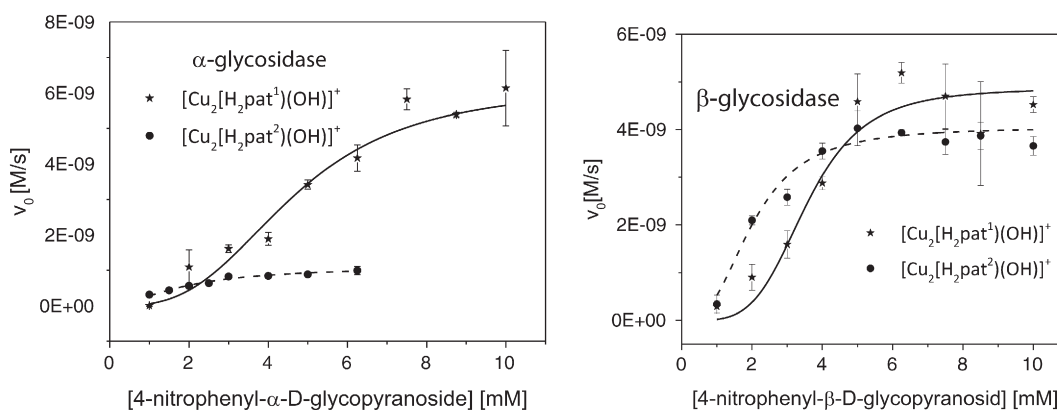


Fig. 4. Michaelis–Menten diagrams of $[\text{Cu}_2(\text{H}_2\text{pat}^1)(\text{OH})]^+$ (**3**, solid), $[\text{Cu}_2(\text{H}_2\text{pat}^2)(\text{OH})]^+$ (**2**, dashed) catalyzed 4-nitrophenyl- α -D-glycopyranoside hydrolysis (pH for the substrate dependence: α -glycosidase: 10.03 $[\text{Cu}_2(\text{H}_2\text{pat}^1)(\text{OH})]^+$, 9.92 $[\text{Cu}_2(\text{H}_2\text{pat}^2)(\text{OH})]^+$ and β -glycosidase: 10.36 $[\text{Cu}_2(\text{H}_2\text{pat}^1)(\text{OH})]^+$, 9.43 $[\text{Cu}_2(\text{H}_2\text{pat}^2)(\text{OH})]^+$).

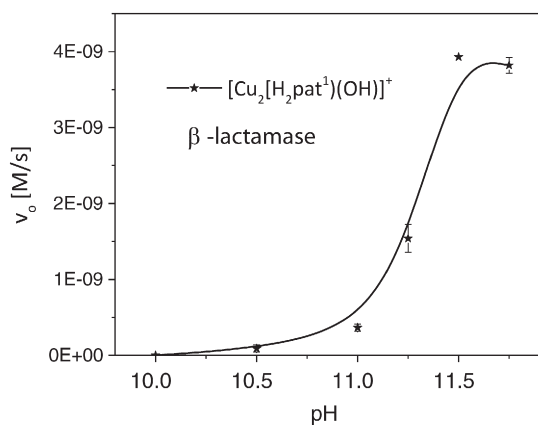


Fig. 5. pH profile of the $[\text{Cu}_2(\text{H}_2\text{pat}^1)(\text{OH})]^+$ (**3**) nitrocefin hydrolysis ($c = 25 \mu\text{M}$; the solid line is a basis spline function and not fit to a kinetic model).

Table 2

Kinetic data from pH-profiles of $[\text{Cu}_2(\text{H}_2\text{pat}^1)(\text{OH})]^+$ (**3**) for the hydrolysis of nitrocefin and the corresponding Michaelis–Menten parameters determined at pH 11.5.

Catalyst	pH _{max}	$v_{0,\text{max}} \cdot 10^{-9}$ [M/s]	$\text{p}K_{\text{a}1}$	$k_{\text{cat}} \times 10^{-4}$ [s ⁻¹]	K_{M} [μM]	$k_{\text{cat}}/K_{\text{M}}$ [M ⁻¹ s ⁻¹]
3	11.50	3.82 ± 0.03	≈ 11.3	$11.34 (\pm 0.91)$	22.47	50.47

shown in Fig. 5 and the resulting kinetic parameters and $\text{p}K_{\text{a}}$ values are summarized in Table 2 (see Supporting Information for a plot of the substrate concentration dependent kinetic data). β -lactamase activity is observed at approx. pH 11 with resulting $k_{\text{cat}}/K_{\text{M}} = 50.5 \text{ M}^{-1} \text{ s}^{-1}$, and this is consistent with similar dinuclear model complexes [7]. The uncatalyzed background rate constant for β -lactam hydrolysis is $k_{\text{uncat}} = 0.025 \cdot 10^{-4} \text{ s}^{-1}$ [24], and the rate enhancement therefore is $k_{\text{cat}}/k_{\text{uncat}} = 454$. The kinetic Michaelis–Menten data reported for natural β -lactamase activity is reported to be in the range of $K_{\text{M}} = 16\text{--}100 \mu\text{M}$ and $k_{\text{cat}} = 0.3\text{--}200 \text{ s}^{-1}$ for *Bacteroides fragilis* and *Aeromonas hydrophila* respectively (substrate nitrocefin) [25].

3. Conclusions

The patellamide-dicopper(II) complexes are among the few examples of dinuclear copper(II) complexes acting as glycosidase-like model compounds. Taking into account the broad reactivity pattern of these compounds with respect to hydrolysis reactions, namely phosphatase, carboanhydrase, glycosidases as well as β -lactamase, several questions emerge. First and probably foremost, it is uncertain whether the catalytic activities observed for the dinuclear copper(II) complexes can be associated with the function of the cyclic peptides in *Prochloron* or *Lissoclinum patellum*. Currently, we are therefore carrying out *in vivo* studies towards an understanding of the stability of dinuclear copper(II) complexes with these naturally occurring ligands. Second and not less important is the question, whether all of the hydrolyses are of importance for the symbiosis partners. Is each of the reactions happening in a separate compartment in the cyanobacterium, providing the optimum pH value? Or is none of these reactions observed in the test tube actually metabolically relevant for the ascidians?

These questions are in the focus of ongoing research. If glycosidase as well as carboanhydrase activity in the cell were mediated by the same dinuclear copper(II) patellamide complexes, this would indicate that the same enzyme is capable of fixing carbon from CO_2 as well as to catabolize the products from the assimilation (Calvin cycle). Here, research has to be carried out as to where which reaction takes place. *Prochloron* might be responsible for the fixation, whereas the ascidian might require the catabolic glycosidase activity.

4. Experimental section

All solvents and reagents (absolute, p.a. grade and *purum* grade) were obtained commercially and used without further purification. Dry solvents were kept above molecular sieves. MilliQ water ($R > 18\text{M}\Omega$) was used for the kinetic assays.

4.1. Ligands and complexes

The cyclic pseudo-peptides were prepared according to [4,6,19].

4.2. Hydrolase assays

4.2.1. Preparation of the multicomponent buffer solutions

The aqueous buffer consisted of CAPS, *N*-cyclohexyl-3-amino-propanesulfonic acid, $\text{p}K_{\text{a}} = 10.40$, CHES, 2-(*N*-cyclohexylamino) ethanesulfonic acid, $\text{p}K_{\text{a}} = 9.30$, HEPES, 4-(2-hydroxyethyl)-1-piperazineethanesulfonic acid, $\text{p}K_{\text{a}} = 7.55$ and MES, 2-(*N*-morpholino) ethanesulfonic acid, $\text{p}K_{\text{a}} = 6.15$. Lithium perchlorate was added to achieve a constant ionic strength of $\mu = 0.45$. Each component was dissolved in Milli-Q water. A standard solution with 55.56 mM of the buffer components and 277.8 mM lithium perchlorate was prepared. Aliquots of 45 mL of the standard buffer were adjusted to the desired pH value by addition of 2 M NaOH. A Metrom 713 pH meter which is equipped with a KCl electrode was used to adjust pH values at 25 °C. The pH-meter was calibrated with pH standard solutions at pH values of 4, 7 and 9. Subsequently the aliquotes were filled up to 50 mL leading to a final buffer concentration of 50 mM and 250 mM lithium perchlorate. Metal ions were removed by stirring adjusted buffers over night with Chelex 100, which was afterwards filtered off by using 45 μm syringe filters. Finally all buffers were degassed by flushing N_2 through the solution in an ultrasonic bath for 3 h in order to remove potentially dissolved CO_2 .

4.2.2. Glycosidase-like activity

The glycosidase-like activity was determined by measuring the hydrolysis of 4-nitrophenyl- α -*D*-glucopyranoside and 4-nitrophenyl- β -*D*-glucopyranoside hydrolysis. The hydrolysis product 4-nitrophenol was produced which could be detected by monitoring the increase of an strong absorbance at 410 nm (ϵ is pH dependent).

Initially, the extinction coefficients of the product formation of 4-nitrophenolate in a multicomponent buffer were calculated by calibration curves for each pH value (pH = 5.5–11.5) using Lambert Beer's law (Table 1). The extinction coefficients of pH = 8.7–11.5 are similar to those determined for 4-nitrophenolate in CAPS buffer ($\epsilon = 16,190 \text{ M}^{-1} \text{ cm}^{-1}$) [10]. The obtained extinction coefficients (see Supporting Information) were used to convert the absorbance of the reaction product into molar amounts.

UV-Vis-spectra data were recorded on a Jasco V-570 spectrophotometer equipped with a Jasco ETC-505 T cryostat at 25 °C and in a 0.3: 1.3: 1 MeCN:buffer:MeOH solution. Using time-course measurements at fixed wavelengths ($\lambda_{\text{max}} = 410 \text{ nm}$), spectrophotometric titrations were performed with a cyclic *pseudo*-peptide concentration of 1 mM (MeOH_{dry}). $\text{Cu}^{\text{II}}(\text{CF}_3\text{SO}_3)_2$ (25 mM, MeOH_{dry}) and base (*n*-Bu₄N)(OMe) (25 mM, MeOH_{dry}) were added to different pH-samples. The final concentrations of dicopper(II) complexes of H_4pat^1 and H_4pat^2 in the cuvette were 40 μM . All solutions were degassed and kept under argon at 7 °C. Blank tests, the autohydrolysis of 4-nitrophenyl- α -*D*-glucopyranoside or 4-nitrophenyl- β -*D*-glucopyranoside respectively, were subtracted from the reported kinetic rates. For the determination of pH dependent reaction velocities the substrate concentration of 30 mM (MeOH_{dry}) was chosen. For substrate dependency measurements at constant pH the substrate concentration was varied between 1 and 50 mM.

4.2.3. β -Lactamase-like activity

The β -lactamase-like activity was determined by measuring the hydrolysis of nitrocefin. The hydrolysis product was produced which could be detected by monitoring the decrease of a strong absorbance of nitrocefin at 390 nm monitored over a period of 420 s, whereas during the initial 120 s the equilibrium was reached, which is why these data have not been used. As nitrocefin, as well as its hydrolysis product show absorption at 390 nm, a corrected extinction coefficient was used $13,415 \text{ M}^{-1} \text{ cm}^{-1}$. UV-Vis-spectra data were recorded on a Jasco V-570 spectrophotometer equipped with a Jasco ETC-505 T cryostat at 37°C and in a 1:1 MeCN:buffer solution. Using time-course measurements at fixed wavelengths ($\lambda_{\text{max}} = 390 \text{ nm}$), spectrophotometric titrations were performed with a cyclic *pseudo*-peptide concentration of 1 mM (MeCN_{dry}). $\text{Cu}^{\text{II}}(\text{CF}_3\text{SO}_3)_2$ (25 mM, MeCN_{dry}) and base (n-Bu₄N)(OMe) (25 mM, MeCN_{dry}) were added to different pH-samples. The final concentrations of dicopper(II) complexes of H₄pat¹ and H₄pat² in the cuvette were $5 \mu\text{M}$. All solutions were degassed and kept under argon. Blank tests, the autohydrolysis of nitrocefin, were subtracted from the reported kinetic rates. For the determination of pH dependent reaction velocities the substrate concentration of $25 \mu\text{M}$ was chosen.

Analogous to glycosidase activity measurements, initially the optimum pH range for lactamase activity was determined. The pH-dependence of the catalysis rates were measured in steps of 0.5 pH units or smaller from pH = 9.0 to pH = 12.0. Subsequently Michaelis-Menten measurements were carried out at the optimum pH value of 11.5. For substrate dependency measurements at constant pH the substrate concentration was varied between 10 and $50 \mu\text{M}$.

Time dependent UV/Vis spectra monitoring β -lactamase-like activity were recorded on a J&M Tidas II with the program Spectralysis 2.0 using an external cryostat Q-Blue Wireless Temperature Control in the range between 300 and 850 nm. These spectra were recorded at 37°C at pH 11.5 with a nitrocefin concentration of $40 \mu\text{M}$ and a complex concentration of $5 \mu\text{M}$ for 20 min at time intervals of $\Delta t = 46.7 \text{ s}$ (see Supporting Information). The resulting spectra were corrected by subtraction the obtained spectrum of the complex.

4.3. DFT Calculations

Fully optimized molecular structures were obtained through geometry optimizations employing the B3LYP [26] functional in conjunction with the def2-tzvp basis set [27]. All calculations were performed with Gaussian 09 [28]. Solvation was approximated by the polarizable continuum model [29] with the permittivity set to methanol. Single point energy and frequency calculations were carried out on the optimized structures. All pictures of computed structures were produced with Avogadro [30].

Acknowledgements

We are grateful for the computational resources provided by the bwForCluster JUSTUS, funded by the Ministry of Science, Research and Arts and the Universities of the State of Baden-Württemberg, Germany, within the framework program bwHPC-C5 as well as for the bwGRID Cluster, funded by the Ministry of Education and Research BMBF. Financial support by the German Science Foundation (DFG), the

Heidelberg Graduate School of Computational Methods for the Sciences (HGS) and the University of Heidelberg are gratefully acknowledged.

Appendix A. Supplementary data

The Supporting Information includes the cartesian coordinates, a list of selected bond lengths and angles of the structures discussed (**1**, **2**) and details on the kinetic studies. Supplementary data associated with this article can be found in the online version, at <http://dx.doi.org/10.1016/j.jinorgbio.2016.02.014>.

References

- [1] W.E. Houssen, J. Koehnke, D. Zollman, J. Vendome, A. Raab, M.C.M. Smith, J.H. Naismith, M. Jaspars, *ChemBiochem* 13 (2012) 2683–2689.
- [2] J. Koehnke, A. Bent, W.E. Houssen, D. Zollman, F. Morawitz, S. Shirran, J. Vendome, A.F. Nneoyiegbu, L. Trembleau, C.H. Botting, M.C.M. Smith, M. Jaspars, J.H. Naismith, *Nat. Struct. Mol. Biol.* 19 (2012) 767–773.
- [3] P. Comba, N. Dovalil, L.R. Gahan, G.R. Hanson, M. Westphal, *Dalton Trans. (Dalton Perspective)* 43 (2014) 1935–1956.
- [4] G. Haberhauer, F. Rominger, *Eur. J. Org. Chem.* (2003) 3209–3218.
- [5] G. Haberhauer, *Tetrahedron Lett.* 49 (2008) 2421.
- [6] P. Comba, N. Dovalil, L.R. Gahan, G. Haberhauer, G.R. Hanson, C.J. Noble, B. Seibold, P. Vadivelu, *Chem. Eur. J.* 18 (2012) 2578–2590.
- [7] P. Comba, L.R. Gahan, G.R. Hanson, M. Westphal, *Chem. Commun.* 48 (2012) 9364–9366.
- [8] P. Comba, L.R. Gahan, G.R. Hanson, M. Maeder, M. Westphal, *Dalton* 43 (2014) 3144–3152.
- [9] P.V. Bernhardt, P. Comba, T.W. Hambley, S.S. Massoud, S. Stebler, *Inorg. Chem.* 31 (1992) 2644–2651.
- [10] S. Striegler, N.A. Dunaway, M.G. Gichinga, J.D. Barnett, A.G.D. Nelson, *Inorg. Chem.* 49 (2010) 2639–2648.
- [11] S. Striegler, M. Dittel, R. Kalso, N.A. Alonso, E.C. Duin, *Inorg. Chem.* 50 (2011) 8869.
- [12] S. Striegler, J.D. Barnett, N.A. Dunaway, *ACS Catal.* 2 (2012) 50.
- [13] J.D. Barnett, S. Striegler, *Top. Catal.* 55 (2012) 460.
- [14] S. Haldar, A.K. Patra, M. Bera, *RSC Adv.* 4 (2014) 62851–62861.
- [15] C.S. Rye, S.G. Withers, *Curr. Opin. Chem. Biol.* 4 (5) (2000) 573–580.
- [16] S.H. Khan, R.A. O'Neill, *Modern Methods in Carbohydrate Synthesis*, Harwood Academic Publishers, Amsterdam, The Netherlands, 1996.
- [17] C. Bebrone, *Biochem. Pharmacol.* 74 (2007) 1686.
- [18] L. Daumann, G. Schenk, L.R. Gahan, *Eur. J. Inorg. Chem.* (2014) 2869–2885.
- [19] G. Haberhauer, A. Pinter, T. Oeser, F. Rominger, *Eur. J. Org. Chem.* (2007) 1779–1792.
- [20] P. Comba, N. Dovalil, G.R. Hanson, G. Linti, *Inorg. Chem.* 50 (2011) 5165–5174.
- [21] I.H. Segel, *Enzyme Kinetics - Behavior and Analysis of Rapid Equilibrium and Steady-State Enzyme Systems*, Wiley-VCH, New York, 1975.
- [22] F. Ortega-Caballero, C. Rousseau, B. Christensen, T.E. Petersen, M. Bols, *J. Am. Chem. Soc.* 127 (2005) 3238–3239.
- [23] J.B. Kempton, S.G. Withers, *Biochemistry* 31 (1992) 9961–9969.
- [24] W.J. Song, F.A. Tezcan, *Science* 346 (2014) 1525–1528.
- [25] A. Felici, G. Amicosante, A. Oratore, R. Strom, P. Ledent, B. Joris, L. Fanuel, J.M. Frere, *Biochem. J.* 291 (1993) 151–155.
- [26] A.D. Becke, *J. Chem. Phys.* B 98 (1993) 5648.
- [27] A. Schäfer, H. Horn, R. Ahlrichs, *J. Chem. Phys.* 97 (1992) 2571–2577.
- [28] M.J. Frisch, G.W. Trucks, H.B. Schlegel, G.E. Scuseria, M.A. Robb, J.R. Cheeseman, G. Scalmani, V. Barone, B. Mennucci, G.A. Petersson, H. Nakatsuji, M. Caricato, X. Li, H.P. Hratchian, A.F. Izmaylov, J. Bloino, G. Zheng, J.L. Sonnenberg, M. Hada, M. Ehara, K. Toyota, R. Fukuda, J. Hasegawa, M. Ishida, T. Nakajima, Y. Honda, O. Kitao, H. Nakai, T. Vreven, J.A. Montgomery Jr., J.E. Peralta, F. Ogliaro, M. Bearpark, J.J. Heyd, E. Brothers, K.N. Kudin, V.N. Staroverov, T. Keith, R. Kobayashi, J. Normand, K. Raghavachari, A. Rendell, J.C. Burant, S. Iyengar, J. Tomasi, M. Cossi, N. Rega, N.J. Millam, M. Klene, J.E. Knox, J.B. Cross, V. Bakken, C. Adamo, J. Jaramillo, R. Gomperts, R.E. Stratmann, O. Yazyev, A.J. Austin, R. Cammi, C. Pomelli, J.W. Ochterski, R.L. Martin, K. Morokuma, V.G. Zakrzewski, G.A. Voth, P. Salvador, J.J. Dannenberg, S. Dapprich, A.D. Daniels, O. Farkas, J.B. Foresman, J.V. Ortiz, J. Cioslowski, D.J. Fox, Gaussian, Gaussian, Inc., Wallingford CT, 2013.
- [29] G. Scalmani, M.J. Frisch, *J. Chem. Phys.* 132 (2010) 114110.
- [30] M.D. Hanwell, D.E. Curtis, D.C. Lonie, T. Vandermeersch, E. Zurek, G.R. Hutchison, *J. Chem. Inf.* 4 (2012) 17.